Adverse roles of mast cell chymase-1 in COPD

Gang Liu [1], Andrew G. Jarnicki [2], Keshav R. Paudel [1], Wenying Lu [3], Ridhima Wadhwa[1], Ashleigh M. Philp[1,4], Hannelore Van Eeckhoutte[5], Jacqueline E. Marshall[1], Vamshikrishna Malyla[1], Angelica Katsifis[1], Michael Fricker [6], Nicole G. Hansbro[1], Kamal Dua[1,7], Nazanin Z. Kermani[8], Mathew S. Eapen [3], Angelica Tiotiu [9,10], K. Fan Chung[9], Gaetano Caramori [11], Ken Bracke[5], Ian M. Adcock [9], Sukhwinder S. Sohal[3], Peter A. Wark [6], Brian G. Oliver[12] and Philip M. Hansbro[1,6]

[1]Centre for Inflammation, Centenary Institute and University of Technology Sydney, School of Life Sciences, Faculty of Science, Sydney, Australia. [2]Department of Pharmacology and Therapeutics, University of Melbourne, Parkville, Australia. [3]Respiratory Translational Research Group, Department of Laboratory Medicine, School of Health Sciences, University of Tasmania, Launceston, Australia. [4]St Vincent's Medical School, University of New South Wales Medicine, University of New South Wales, Sydney, Australia. [5]Laboratory for Translational Research in Obstructive Pulmonary Diseases, Department of Respiratory Medicine, Ghent University Hospital, Ghent, Belgium. [6]Priority Research Centre for Healthy Lungs, Hunter Medical Research Institute, University of Newcastle, Callaghan, Australia. [7]Discipline of Pharmacy, Graduate School of Health, University of Technology Sydney, Ultimo, Australia. [8]Data Science Institute, Department of Computing, Imperial College London, London, UK. [9]National Heart and Lung Institute, Imperial College London, London, UK. [10]Department of Pulmonology, University Hospital of Nancy, Nancy, France. [11]UOC di Pneumologia, Dipartimento di Scienze Biomediche, Odontoiatriche e delle Immagini Morfologiche e Funzionali (BIOMORF), Università di Messina, Messina, Italy. [12]Woolcock Institute and School of Life Science, Faculty of Science Life Science, University of Technology Sydney, Sydney, Australia.

Corresponding author: Philip M. Hansbro (philip.hansbro@uts.edu.au)

Shareable abstract (@ERSpublications)
hCMA1 released from mast cells induces macrophages to release TNF-α in the lung and promotes the pathogenesis of COPD. hCMA1 may be a novel therapeutic target in COPD. https://bit.ly/3b3OkKT

Cite this article as: Liu G, Jarnicki AG, Paudel KR, *et al*. Adverse roles of mast cell chymase-1 in COPD. *Eur Respir J* 2022; 60: 2101431 [DOI: 10.1183/13993003.01431-2021].

This article has an editorial commentary: https://doi.org/10.1183/13993003.01356-2022

Received: 20 May 2021
Accepted: 8 June 2022

Abstract

Background COPD is the third leading cause of death worldwide. Cigarette smoke (CS)-induced chronic inflammation inducing airway remodelling, emphysema and impaired lung function is the primary cause. Effective therapies are urgently needed. Human chymase (hCMA)1 and its orthologue mCMA1/mouse mast cell protease (mMCP)5 are exocytosed from activated mast cells and have adverse roles in numerous disorders, but their role in COPD is unknown.

Methods We evaluated hCMA1 levels in lung tissues of COPD patients. We used *mmcp5*-deficient ($^{-/-}$) mice to evaluate this protease's role and potential for therapeutic targeting in CS-induced experimental COPD. In addition, we used *ex vivo/in vitro* studies to define mechanisms.

Results The levels of hCMA1 mRNA and CMA1^{+} mast cells were increased in lung tissues from severe compared to early/mild COPD patients, non-COPD smokers and healthy controls. Degranulated mast cell numbers and mMCP5 protein were increased in lung tissues of wild-type mice with experimental COPD. *mmcp5*$^{-/-}$ mice were protected against CS-induced inflammation and macrophage accumulation, airway remodelling, emphysema and impaired lung function in experimental COPD. CS extract challenge of co-cultures of mast cells from wild-type, but not *mmcp5*$^{-/-}$ mice with wild-type lung macrophages increased in tumour necrosis factor (TNF)-α release. It also caused the release of CMA1 from human mast cells, and recombinant hCMA-1 induced TNF-α release from human macrophages. Treatment with CMA1 inhibitor potently suppressed these hallmark features of experimental COPD.

Conclusion CMA1/mMCP5 promotes the pathogenesis of COPD, in part, by inducing TNF-α expression and release from lung macrophages. Inhibiting hCMA1 may be a novel treatment for COPD.

Introduction

COPD affects >300 million people globally [1]. Cigarette smoke (CS)-induced chronic inflammation is the major cause; however, air pollution, bushfire smoke and genetic factors contribute [2]. Pulmonary

inflammation in COPD is characterised by increased neutrophils, macrophages, lymphocytes and mast cells. These changes lead to small-airway remodelling and alveolar destruction and emphysema [3], airflow limitation, impaired lung function and severe breathing difficulties, often leading to death [4]. Current treatments aim to reduce symptoms and do not halt or reverse the progression of COPD. A deeper understanding of pathogenesis will enable the identification of new therapeutic targets, and the development of new therapies.

Mast cells are potent multifunctional immune cells that reside in the lung and other organs. Mast cell committed progenitors are generated in the bone marrow and fetal liver. They reach their target organs *via* the circulation, where they complete their differentiation and maturation [5]. Mast cells are major contributors to innate and acquired immunity [5], and are first-line responders to insults like CS [6]. Mast cell secretory granules contain pre-formed mediators, including tryptases and chymases that have potent immune bioactivities. Exposure to foreign particles induce mast cells to degranulate and release their pre-formed pro-inflammatory mediators [7]. We previously demonstrated adverse roles for mast cells and their granule tryptases in the pathogenesis of CS-induced experimental COPD [8–11]. Another prominent protease in human mast cells is chymase-1 (hCMA1; GenBank GeneID 1215) [12]. The human and mouse genome consortia concluded that mouse mast cell protease (mMCP)5 (gene ID 17226) is the orthologue of hCMA1 [13], even though mouse mast cells (mMCs) express additional related proteases [14]. Furthermore, mCMA1/mMCP5 is packaged in granules of mMCs with heparin proteoglycans and mouse carboxypeptidase-A3 (mCPA3), as is hCMA1 in human mast cells.

Mouse and human CMA1 have important roles in numerous inflammatory disorders, including cardiovascular and pulmonary diseases [15]. hCMA1 can mediate the conversion of angiotensin (Ang)-I to Ang-II, and inhibiting Ang-II reduces blood pressure and protects against cardiovascular and metabolic disorders [15]. Increased numbers of mast cells occur in the lung fluids and tissues of COPD patients [16]. hCMA1^{+} mast cells are increased in the lungs of severe Global Initiative for Chronic Obstructive Lung Disease (GOLD) stage IV COPD patients [17]. Inhibiting mouse chymases reduced pulmonary hypertension and fibrosis in an experimental model of lung injury [18]. Nevertheless, the roles of mouse and human CMA1 in COPD are unknown.

We show that hCMA1 transcripts and CMA1^{+} mast cells are increased in bronchial biopsies and lung tissues from COPD patients compared to controls. We demonstrate that our *mmcp5*-deficient ($^{-/-}$) mice are protected against the development of CS-induced experimental COPD. We also show that CS extract (CSE) induces mMCP5/CMA1 release from mast cells which promotes macrophage lung accumulation and tumour necrosis factor (TNF)-α production from mouse and human cells. Pharmacological inhibition of mCMA1/mMCP5 suppressed the hallmark features of experimental COPD, suggesting that targeting hCMA1 may be therapeutically beneficial.

Methods

Detailed descriptions are as described previously, and in the supplementary material [3, 8, 10–12, 19–25].

Results

Chymase-1 mRNA levels are increased in the lungs of COPD patients

To define the role of hCMA1 in COPD, we first assessed its mRNA levels in bronchial biopsies from mild COPD patients (GOLD stages I–II), non-COPD smokers and nonsmoking healthy controls in an existing dataset (GSE8545) [26]. Levels were not significantly different between groups (figure 1a). However, in another microarray dataset (GSE5058) [27] *hCMA1* mRNA levels were significantly increased in severe COPD patients (GOLD stages III–IV) compared to both non-COPD smokers (p=0.011) and healthy controls (p=0.049; figure 1b). To confirm the association with severe rather than mild COPD, we next assessed levels in lung biopsies from lung healthy and non-COPD smoker controls and mild (GOLD I–II) and severe (III–IV) COPD patients in another larger validation dataset (GSE37147) [28]. *hCMA1* mRNA levels were again not different in mild COPD patients, but were significantly increased in severe COPD patients compared to controls (p=0.017; figure 1c). *hCMA1* mRNA levels were significantly increased in lung tissues from severe COPD patients (combined GSE38974 and GSE69818), there was no difference between GOLD III and IV (figure 1d).

Mast cells and CMA1^{+} mast cells are increased in the lungs of COPD patients

Mast cell gene signatures derived from single-cell (sc)RNA-sequencing (seq) analysis [29, 30] were enriched in COPD lung tissue compared to healthy control subjects and reached significance in GOLD stage IV subjects (p=0.04; supplementary table S2). Previous data suggest that this reflects more mast cells in asthmatic bronchial biopsy tissue than in healthy control tissue [29]. In addition, there was a significant

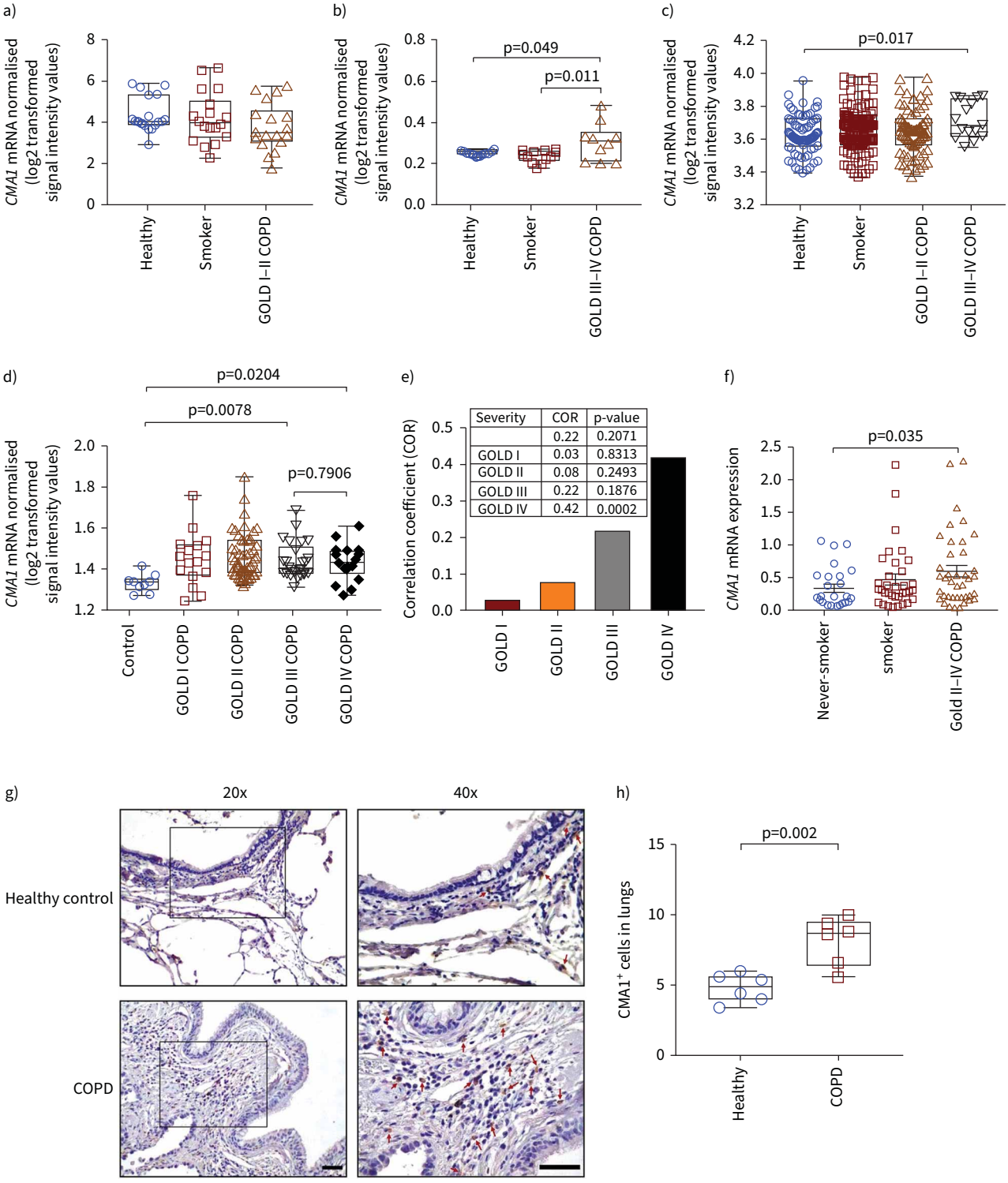

FIGURE 1 Chymase (CMA)1 mRNA levels, mast cells (MCs) and CMA1$^+$ MCs are increased in the lungs of COPD patients. a) Human *(h)CMA1* mRNA levels in bronchial biopsies from lung healthy controls (n=18), non-COPD smokers (n=18) and mild Global Initiative for Chronic Obstructive Lung Disease (GOLD) stage I–II COPD patients (n=18 for each group) in an existing microarray dataset (GSE8545). b) *hCMA1* mRNA levels were measured in bronchial biopsies from lung healthy controls (n=12), non-COPD smokers (n=12) and severe GOLD stage III–IV COPD patients (n=15) in another existing microarray dataset (GSE5058). c) *hCMA1* mRNA levels were measured in bronchial biopsies from lung healthy controls (n=73), non-COPD smokers (n=100) and mild GOLD I–II (n=67) and severe GOLD III–IV (n=15) COPD patients in another existing microarray dataset (GSE37147). d) *hCMA1* mRNA transcript levels in two combined datasets (GSE38974 and GSE69818) from lung tissues from controls (n=9), COPD patients with GOLD I (n=12), II (n=26), III (n=7) and IV (n=19). e) Correlation between *hCMA1* and MC signatures in combined single-cell RNA-sequencing data

(GSE38974 and GSE69818) from lung tissues from COPD patients with GOLD I (n=16), II (n=49), III (n=9) and IV (n=19). f) *hCMA1* mRNA transcript levels in lung tissues from never-smokers (n=26), smokers without COPD (n=34) and COPD patients with GOLD II–IV (n=40) by quantitative PCR. g) Human lung sections from healthy controls (n=6) and COPD patients (n=6) were stained with CMA1 by immunohistochemistry, and h) $CMA1^+$ mast cells were enumerated. Scale bars=100 μm in both 20× and 40× magnifications. Data are presented as mean±SEM. Statistical differences were determined using one-way ANOVA with Bonferroni post-test.

correlation between the enrichment scores for these scRNA-seq mast cell signatures and CMA1 expression according to GOLD stage (figure 1e).

To validate the increases in CMA1 expression in lung tissue, we measured its transcript levels in lung samples by quantitative (q)PCR. We found that CMA1 mRNA levels were significantly increased in lung samples from COPD GOLD stage II–IV patients compared to never-smokers (figure 1f and supplementary table S3). Several previous studies showed that $hCMA1^+$ mast cells are increased in lungs from COPD patients compared to healthy donors [17, 31]. Notably, we confirmed this by immunohistochemistry and showed that $CMA1^+$ mast cells were significantly increased in lung tissues from COPD patients (figure 1g) compared to healthy control lungs (figure 1h).

Degranulated mast cells and mMCP5 protein are increased in the lungs in CS-induced experimental COPD

We next used our well-established nose-only CS-induced experimental model of COPD to examine the role of mCMA1/mMCP5 in pathogenesis [3, 8–11, 21]. Lungs were collected from wild-type C57BL/6 mice after 8 weeks of CS exposure, when the major hallmark features of human COPD (chronic airway inflammation, airway remodelling/fibrosis, emphysema-like alveolar enlargement, impaired lung function) have developed. The levels of CS exposure are representative of a pack-a-day human smoker. Lung sections were stained with chloroacetate esterase to detect activated mast cells that had degranulated (figure 2a). Mast cell numbers were substantially increased (more than three-fold) after 8 weeks of CS exposure compared to normal air-exposed controls (figure 2a and b). These mast cells showed more degranulation when exposed to CS (figure 2c). Mast cells were localised in the lung parenchyma of control mice, but these cells (degranulated mast cells) were located close to blood vessels and airways in experimental COPD (supplementary figure S1). The levels of mCMA1/mMCP5 gene (supplementary figure S2a) and protein (figure 2d and e) were significantly increased in the lungs in experimental COPD. CS exposure increased $mMCP5^+$ and $mMCP6^+$ mast cells in the lungs in experimental COPD, with greater increases in $mMCP5^+$ mast cells (figure 2f–h). These cells also shifted from the parenchyma to connective tissues close to blood vessels and airways after 8 weeks' CS exposure. There are five chymase paralogues in mice and *mcpt* is the gene name for mMCPs. The sequence for *mcpt3* does not exist, and so we assessed the expression of the others (*mcpt1/2/4*) in the lungs in experimental COPD. CS exposure increased *mcpt1* mRNA transcript levels, but did not change those of *mcpt2* and *mcpt4* (supplementary figure S2b–d). *mcpt5* gene expression was also increased in mouse livers after 8 weeks of CS exposure, but *mmcpt2* and *4* levels were unchanged (supplementary figure S2e–g).

Generation of $mmcp5^{-/-}$ *C57BL/6 mice*

Transgenic $mmcp5^{-/-}$ mice were generated by replacing intron 2 and exon 3 of the *mmcp5* gene with the Neo^r gene [12]. We further characterised these mice by showing that the exon 3 DNA fragment of the *mmcp5* gene in $mmcp5^{-/-}$ mice was larger than in wild-type mice due to the insertion of the Neo^r gene (figure 3a). Additionally, we showed that mMCP5 protein was detectable in lung extracts from wild-type, but not $mmcp5^{-/-}$ mice by immunoblot (figure 3b and supplementary figure S3a). We also isolated and cultured mouse bone marrow-derived mast cells (mBMMCs) from wild-type and $mmcp5^{-/-}$ mice and confirmed their identity with chloroacetate esterase staining (figure 3c). mBMMCs from wild-type but not $mmcp5^{-/-}$ mice contained mMCP5 protein (figure 3d). Furthermore, mMCP5 protein was detected in mBMMC lysates from wild-type but not $mmcp5^{-/-}$ mice (figure 3e and supplementary figure S3b).

$mmcp5^{-/-}$ *mice have reduced pulmonary macrophages in experimental COPD*

Next, we assessed pathogenesis in the lungs in wild-type compared to $mmcp5^{-/-}$ mice exposed to CS for 8 weeks. Bronchoalveolar lavage fluid (BALF) was collected and total and differential leukocyte counts determined. Wild-type mice had increased numbers of total leukocytes in experimental COPD compared to normal air-exposed controls. In contrast, $mmcp5^{-/-}$ mice had significantly reduced total leukocytes compared to wild-type mice with experimental COPD, although numbers were still higher than air-exposed wild-type and $mmcp5^{-/-}$ controls (figure 4a). Differential counts showed that macrophages, neutrophils and lymphocytes were the predominant cells and were increased in the airways of wild-type mice with

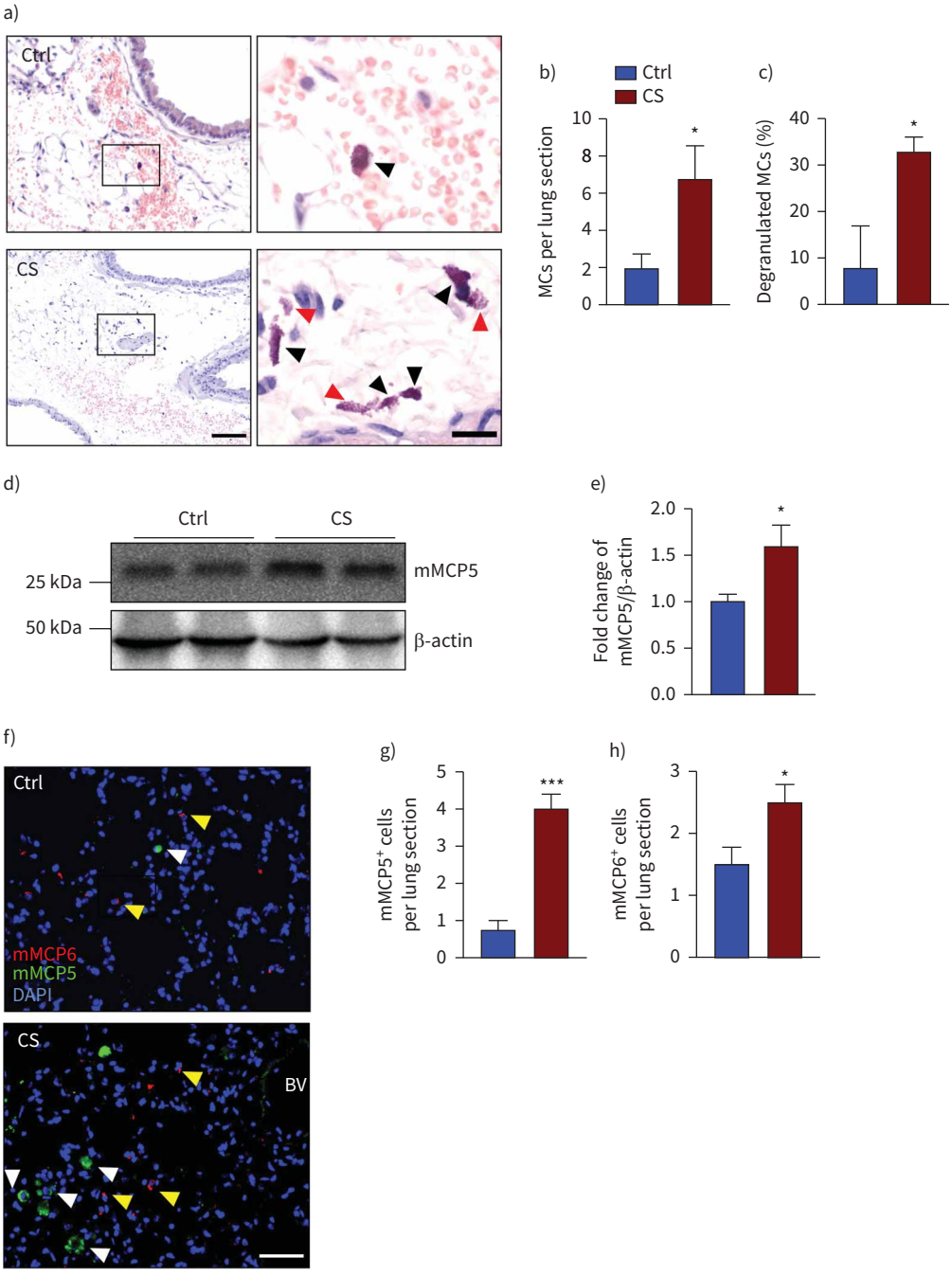

FIGURE 2 Mast cell (MC) numbers and mouse mast cell protease (mMCP)5 proteins are increased in the lungs in experimental COPD. Mice were exposed to 8 weeks of cigarette smoke (CS); controls (Ctrl) were exposed to normal air. a) Lung tissues were collected and stained with chloroacetate esterase to identify degranulating MCs. Images were taken using light microscopy. Scale bars=100 μm (left); 20 μm (right). Black arrowheads indicate MCs; red arrowheads indicate MC degranulation. b) Total MC numbers and c) percentage of degranulated MCs were enumerated in the whole lung sections stained with chloroacetate esterase. d) Total proteins were extracted from mouse lungs and mMCP5 protein was detected by immunoblot analysis. e) Fold change of densitometry of mMCP5 normalised to β-actin. f) Mouse lung sections stained with mMCP5 (green), mMCP6 (red) and nuclei stained with DAPI (blue) in experimental COPD by immunofluorescence. Scale bars=50 μm. g) $mMCP5^+$ and h) $mMCP6^+$ MCs were enumerated. n=4–6. Data are presented as mean±SEM. Statistical differences were determined using t-test. *: p<0.05, ***: p<0.001.

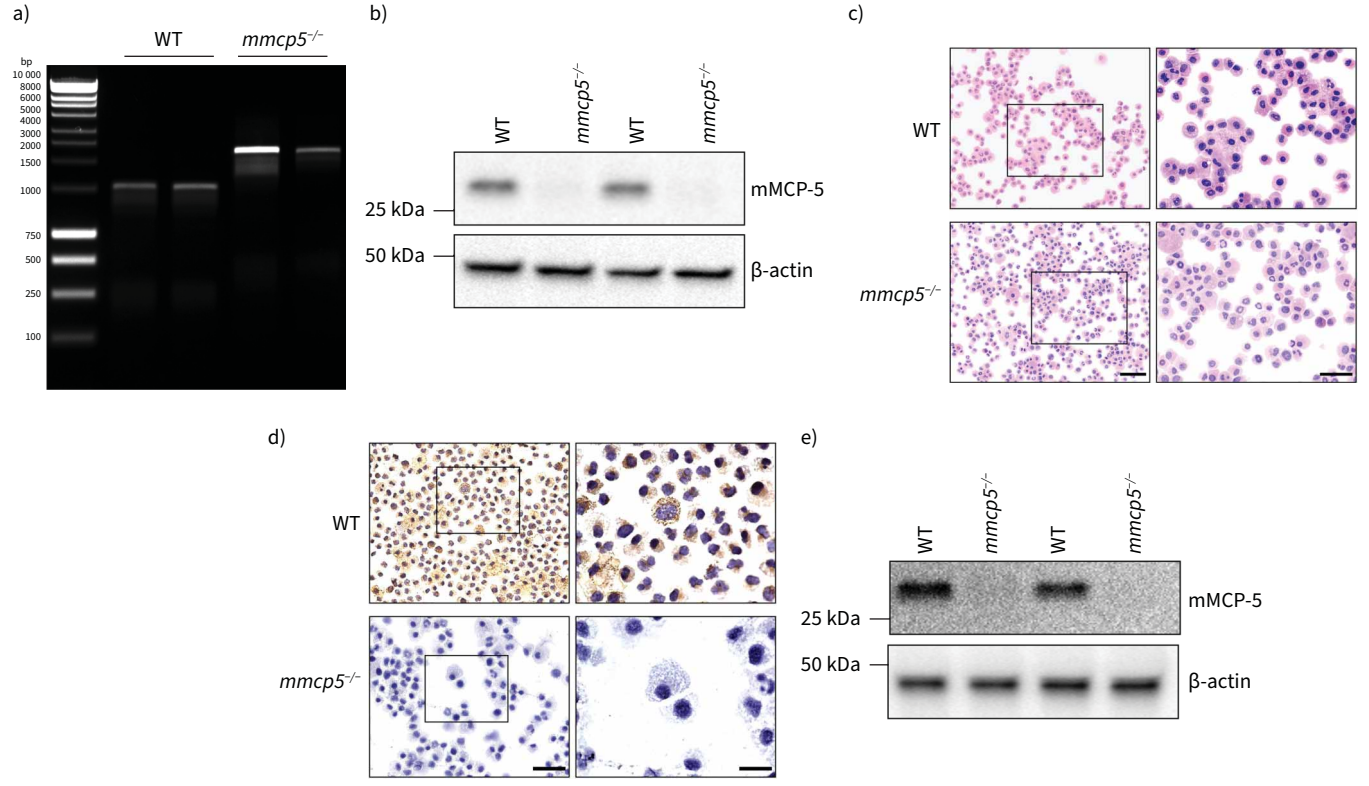

FIGURE 3 Genotyping and mouse mast cell protease (mMCP)5 protein assessment of *mmcp5*$^{-/-}$ mice. a) Genomic DNA was obtained from the tails of wild-type (WT) and *mmcp5*$^{-/-}$ C57BL/6 mice, and a previously described PCR approach was used to genotype the mice. b) Lung proteins were extracted from WT and *mmcp5*$^{-/-}$ mice and mMCP5 protein was detected by immunoblot. Bone marrow derived mast cells (mBMMCs) were generated from WT and *mmcp5*$^{-/-}$ mice. c) Some mBMMCs were cytospun onto histology slides and stained with chloroacetate esterase (scale bar=200 μm; insert shows the expanded image of indicated region, scale bar=50 μm). d) Other mBMMCs were stained with anti-mMCP5 antibody to evaluate their immunohistochemistry (scale bar=200 μm; rectangle indicates high magnification area, scale bar=50 μm). e) mBMMC lysates were extracted from WT and *mmcp5*$^{-/-}$ mice and mMCP5 protein was detected using SDS-PAGE immunoblot.

experimental COPD. The reduced total leukocytes in the BALF of CS-exposed *mmcp5*$^{-/-}$ mice was due primarily to reduced numbers of macrophages (~50%) with no change in other leukocytes. We showed previously that macrophages are critical in experimental COPD pathogenesis and their depletion suppressed disease development [8]. We also found that mast cell numbers were increased in the lungs from wild-type and *mmcp5*$^{-/-}$ mice, but were not different between the two strains (supplementary figure S4).

mmcp5$^{-/-}$ mice have reduced pulmonary TNF-α protein levels in experimental COPD

We assessed the mRNA levels of key pathogenic cytokines and chemokines in mouse lungs using reverse transcriptase qPCR. *Tnfa* mRNA levels were significantly increased in the lungs of wild-type mice with experimental COPD compared to normal air-exposed controls (figure 4b). In contrast, CS- and air-exposed *mmcp5*$^{-/-}$ mice had substantially lower levels of *Tnfa* mRNA that were below baseline expression in air-exposed wild-type mice. In contrast, lung *Cxcl1* mRNA levels were significantly increased and similar between wild-type and *mmcp5*$^{-/-}$ mice after 8 weeks of CS exposure (figure 4c). CS exposure did not change the mRNA expression of other factors important in COPD, mast cell responses and macrophage recruitment; transforming growth factor-β (*Tgfb1*), *Il33*, *Ccl2* and *Il12* in the lungs of wild-type or *mmcp5*$^{-/-}$ mice (figure 4d–g). In addition, we determined TNF-α protein levels by ELISA. CS exposure-induced increased TNF-α protein levels in the lungs of wild-type and *mmcp5*$^{-/-}$ mice compared to air-exposed controls (figure 4h). However, the levels were significantly reduced in CS-exposed *mmcp5*$^{-/-}$ compared to wild-type mice.

mmcp5$^{-/-}$ mice have reduced small-airway remodelling in experimental COPD

Small-airway remodelling is a major intractable feature of COPD. To explore the role of mMCP5 in this process, lung sections from wild-type and *mmcp5*$^{-/-}$ mice were stained with Masson's trichrome to

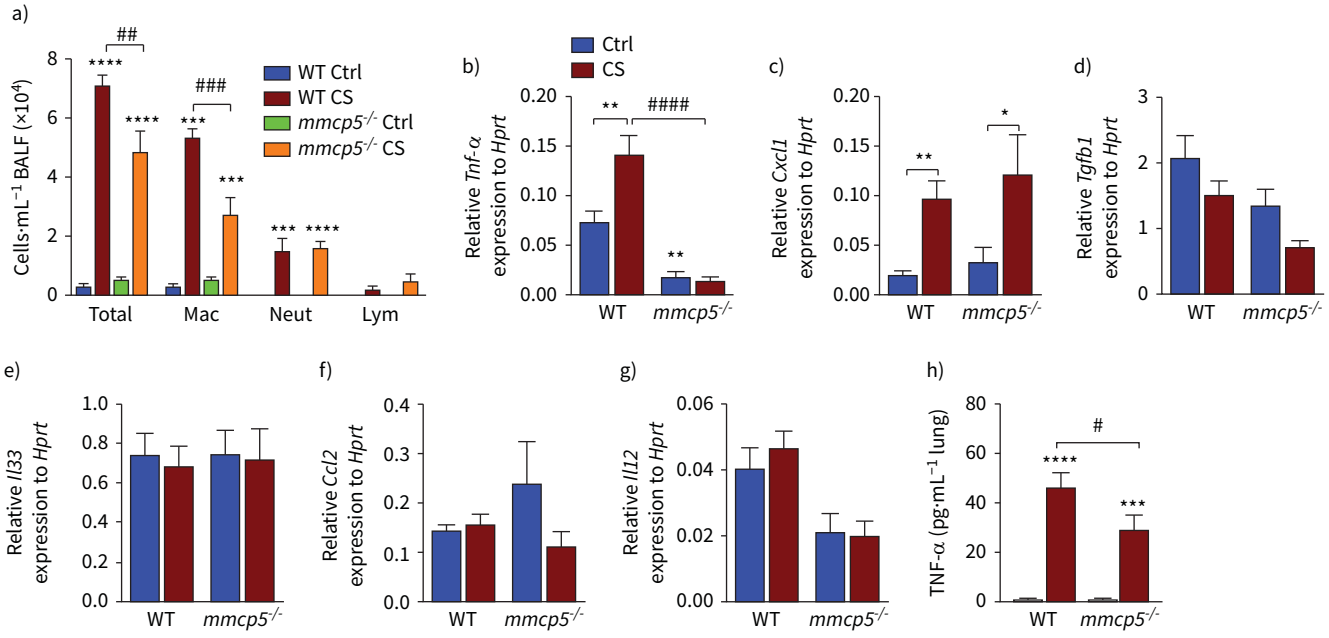

FIGURE 4 Targeted disruption of the mouse mast cell protease (*mmcp5*) gene protects against cigarette smoke (CS)-induced inflammation in experimental COPD. Wild-type (WT) and *mmcp5*$^{-/-}$ mice were exposed to CS or normal air for 8 weeks. a) Differential inflammatory cell counts in bronchoalveolar lavage fluid (BALF). Relative mRNA levels that encode b) *Tnfa*, c) *Cxcl1*, d) *Tgfb1*, e) *Il33*, f) *Ccl2* and g) *Il12* to *Hprt* in mouse lungs by reverse transcriptase quantitative PCR. h) Tumour necrosis factor (TNF)-α protein levels were measured in mouse lungs previously ELISA. n=5–6. Ctrl: control; Mac: macrophages; Neut: neutrophils; Lym: lymphocytes. Data are presented as mean±SEM. Statistical differences were determined using one-way ANOVA with Bonferroni post-test. *: p<0.05, **: p<0.01, ***: p<0.001, ****: p<0.0001 compared to normal air-exposed controls. $^{\#}$: p<0.05, $^{\#\#}$: p<0.01, $^{\#\#\#}$: p<0.001, $^{\#\#\#\#}$: p<0.0001 compared to CS-exposed WT mice.

evaluate histochemically small-airways collagen deposition (figure 5a). Collagen deposition was significantly increased around small airways in wild-type mice with experimental COPD compared to normal air-exposed controls (figure 5b). In contrast, *mmcp5*$^{-/-}$ mice were completely protected against airway fibrosis with levels comparable to baseline in air-exposed controls. CS exposure resulted in epithelial cell thickening in small airways from wild-type mice (figure 5c). However, the absence of mMCP5 protected against epithelial thickening after 8 weeks of CS exposure (figure 5d). CS exposure increased mucus cells around the airways, but the numbers were not different between wild-type and *mmcp5*$^{-/-}$ mice (supplementary figure S5).

mmcp5$^{-/-}$ mice have reduced emphysema in experimental COPD

Emphysema is another major intractable feature and critical disease issue in COPD. To assess the role of mMCP5, alveolar diameter was measured to assess emphysema-like enlargement in wild-type and *mmcp5*$^{-/-}$ mice (figure 5e). 8 weeks of CS exposure increased alveolar diameter in wild-type mice (figure 5f). In contrast, *mmcp5*$^{-/-}$ mice were completely protected against CS-induced alveolar enlargement with significantly lower airspace diameter compared to CS-exposed wild-type mice, with levels similar to baseline in air-exposed controls. Matrix metalloproteinases (MMPs) regulate extracellular matrix degradation which contributes to airway remodelling and emphysema in COPD [32]. CS exposure increased pro- and active-MMP9 proteins in wild-type mouse lungs that was absent in *mmcp5*$^{-/-}$ mice (figure 5g–i).

mmcp5$^{-/-}$ mice are protected against impaired lung function in experimental COPD

We assessed whether the combined effects of reduced pathogenic features affected lung function in *mmcp5*$^{-/-}$ mice. Lung function, in terms of transpulmonary resistance (figure 6a), lung volume (figure 6b) and dynamic compliance (figure 6c) were all increased in wild-type mice with experimental COPD compared to air-exposed controls. These changes were completely inhibited in *mmcp5*$^{-/-}$ mice after CS exposure and were at baseline levels in air-exposed controls. In addition, we measured static lung compliance to assess lung elasticity using pressure–volume loops (figure 6d). Static lung compliance was

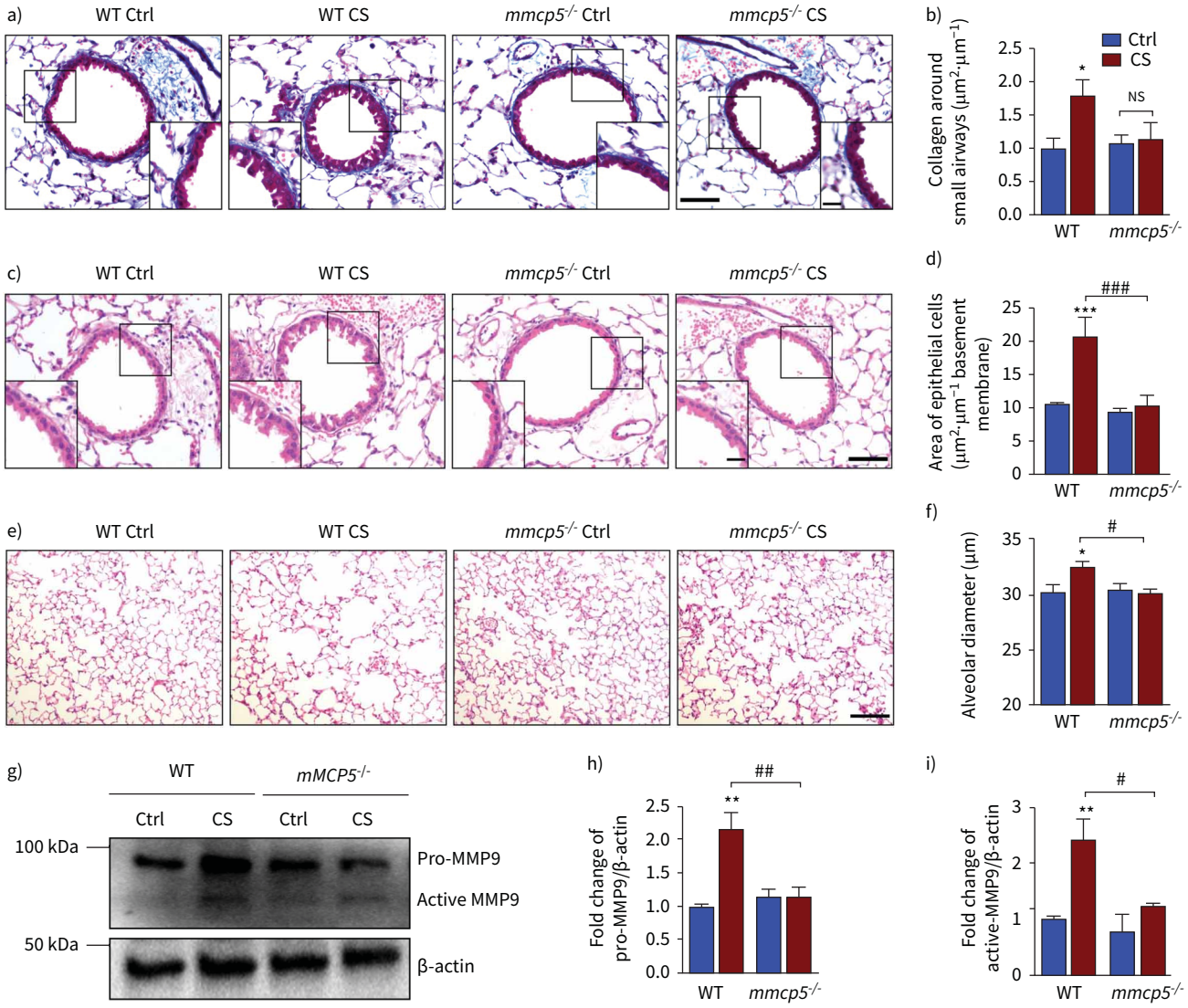

FIGURE 5 Mouse mast cell protease (*mmcp5*) disruption protects against cigarette smoke (CS)-induced small-airway remodelling, emphysema-like alveolar enlargement and reduced matrix metalloproteinase (MMP) protein in experimental COPD. Wild-type (WT) and *mmcp5*$^{-/-}$ mice were exposed to CS or normal air for 8 weeks. a) Collagen deposition around small airways in lung sections was assessed using Masson's trichrome histochemistry (blue colour indicates collagen; scale bar=50 μm; insets show expanded image of indicated region; scale bar=15 μm). b) Quantification of collagen area around the small airways normalised to the perimeter of the basement membrane. c) Mouse lung sections were stained with haematoxylin and eosin (H&E) (scale bar=50 μm; insets show expanded image of indicated region; scale bar=15 μm); and d) quantification of epithelial thickness in the small airways normalised to the perimeter of the basement membrane. e) Mouse lung sections were stained with H&E (scale bar=200 μm) and f) emphysema-like alveolar enlargement was measured by assessment of alveolar diameter. n=5–6. g) Total proteins were extracted from the lungs and pro- and active MMP9 were detected by immunoblot. Fold change of densitometry of h) pro- and i) active MMP9 normalised to β-actin. n=4–6. Ctrl: control; NS: nonsignificant. Data are presented as mean±SEM. Statistical differences were determined using one-way ANOVA with Bonferroni post-test. *: p<0.05, **: p<0.01, ***: p<0.001 compared to normal air-exposed controls. #: p<0.05, ##: p<0.01, ###: p<0.005 compared to CS-exposed WT mice.

increased in wild-type mice with experimental COPD and was comparatively decreased in CS-exposed *mmcp5*$^{-/-}$ mice.

mMCP5 promotes mast cell-induced macrophage production of TNF-α with CSE challenge

We assessed how mCMA1/mMCP5 contributes to experimental COPD pathogenesis. *mmcp5*$^{-/-}$ mice had reduced lung TNF-α mRNA and protein levels after 8 weeks of CS exposure (figure 4). Although mast cells can transiently express TNF-α, macrophages are the main cellular source in the lung [33]. TNF-α has

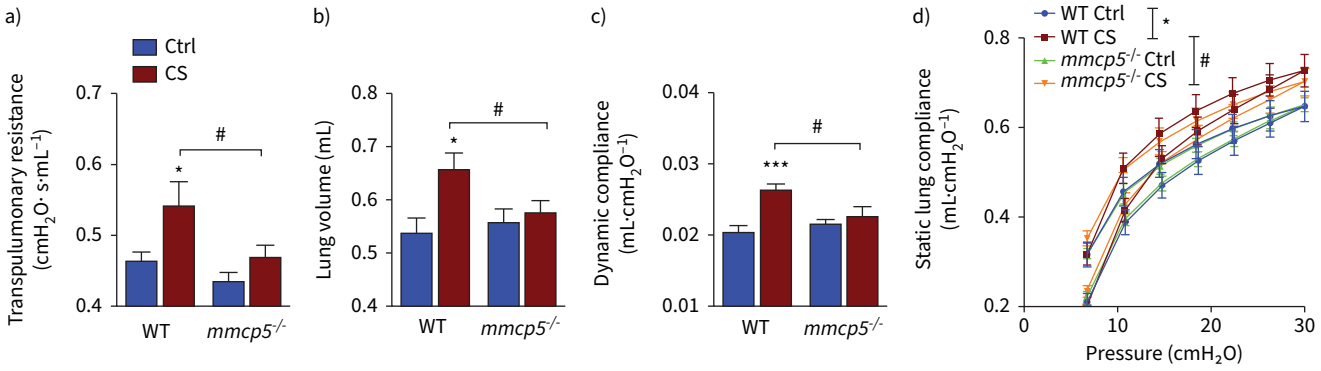

FIGURE 6 Mouse mast cell protease (*mmcp5*) disruption protects against cigarette smoke (CS)-induced impaired lung function in experimental COPD. Wild-type (WT) and *mmcp5*$^{-/-}$ mice were exposed to CS or normal air for 8 weeks. Lung function was measured in terms of a) transpulmonary resistance, b) lung volume, c) dynamic compliance and d) static lung compliance from pressure–volume loops. n=5–6. Data are presented as mean±SEM. Statistical differences were determined using one-way ANOVA with Bonferroni post-test. *: p<0.05, ***: p<0.001 compared to normal air-exposed controls. #: p<0.05 compared to CS-exposed WT mice.

major roles in COPD pathogenesis, and inhibiting its receptors reduces inflammation and emphysema in an experimental model of CS-induced COPD [34]. To further define how mast cells and mCMA1/mMCP5 promotes TNF-α production in COPD, we generated mBMMCs from naïve wild-type and *mmcp5*$^{-/-}$mice (figure 3a). *Ex vivo* differentiated mBMMCs from wild-type mice contained mMCP5 protein, whereas those from *mmcp5*$^{-/-}$ mice did not (figure 3d–e), further confirming the genotype data (figure 3a).

Exposure of macrophages to 5% CSE causes the secretion of TNF-α protein, but this concentration does not affect mast cell viability [35]; therefore, we chose this concentration of CSE for our studies. To identify the optimal time point for CSE exposure of mBMMCs, lung macrophages (Raw246.7) were co-cultured with or without wild-type mBMMCs over a 6–48 h time course of 5% CSE challenge. TNF-α protein levels were measured in lysates by ELISA (supplementary figure S6). Macrophages secreted more TNF-α protein (p=0.071) when co-cultured with wild-type mBMMCs after 12 h of 5% CSE challenge, with a significant increase and peak after 24 h (figure 7a). TNF-α levels were not changed at early (6 h) or later (48 h) time points; therefore, we selected 24 h as the optimal time point. Macrophages and mBMMCs from wild-type and *mmcp5*$^{-/-}$ mice were co-cultured with or without 5% CSE challenge for 24 h, and TNF-α proteins were measured in lysates by ELISA. Macrophages co-cultured with mBMMCs from wild-type mice and exposed to CSE released substantially increased levels (two-fold) of TNF-α compared to media exposure (figure 7b). In contrast, co-cultures with mBMMCs from *mmcp5*$^{-/-}$ mice exposed to CSE did not produce increased TNF-α relative to media-treated controls with levels substantially reduced compared to wild-type mBMMCs. Therefore, mCMA1/mMCP5 is critical for TNF-α production by macrophages in response to CS. In addition, we found that CSE-induced TNF-α protein was reduced in cell supernatants after co-culture with BMMCs from *mmcp5*$^{-/-}$ mice (figure 7c).

To further define the role of mMCP5 in COPD, we assessed the responses of primary alveolar macrophages (supplementary figure S7) from wild-type and *mmcp5*$^{-/-}$ mice challenged with CSE. TNF-α protein levels were significantly increased in macrophages from both wild-type and *mmcp5*$^{-/-}$ mice after challenge (figure 7d). Then wild-type alveolar macrophages were co-cultured with BMMCs from wild-type and *mmcp5*$^{-/-}$ mice with or without CSE. CSE induced TNF-α protein responses in macrophages co-cultured with wild-type but not *mmcp5*$^{-/-}$ BMMCs (figure 7e).

In addition, CSE challenge increased CMA1 protein levels in human mast cells (figure 7f) and cell supernatant (figure 7g). Furthermore, recombinant hCMA1 protein increased TNF gene expression (figure 7h) and protein levels in supernatants of human macrophages (figure 7i). These findings confirmed the mechanism whereby CS induced CMA1 release from mast cells which increased TNF production by macrophages (figure 7g).

Therapeutic inhibition of CMA1 in mice reduces inflammation, small-airway remodelling, emphysema and impaired lung function in experimental COPD

BMMCs from wild-type mice were co-cultured with macrophages. Cell were challenged with 5% CSE and treated with CMA1 inhibitor. Substantial increases in CSE-induced TNF protein levels in cell lysates were

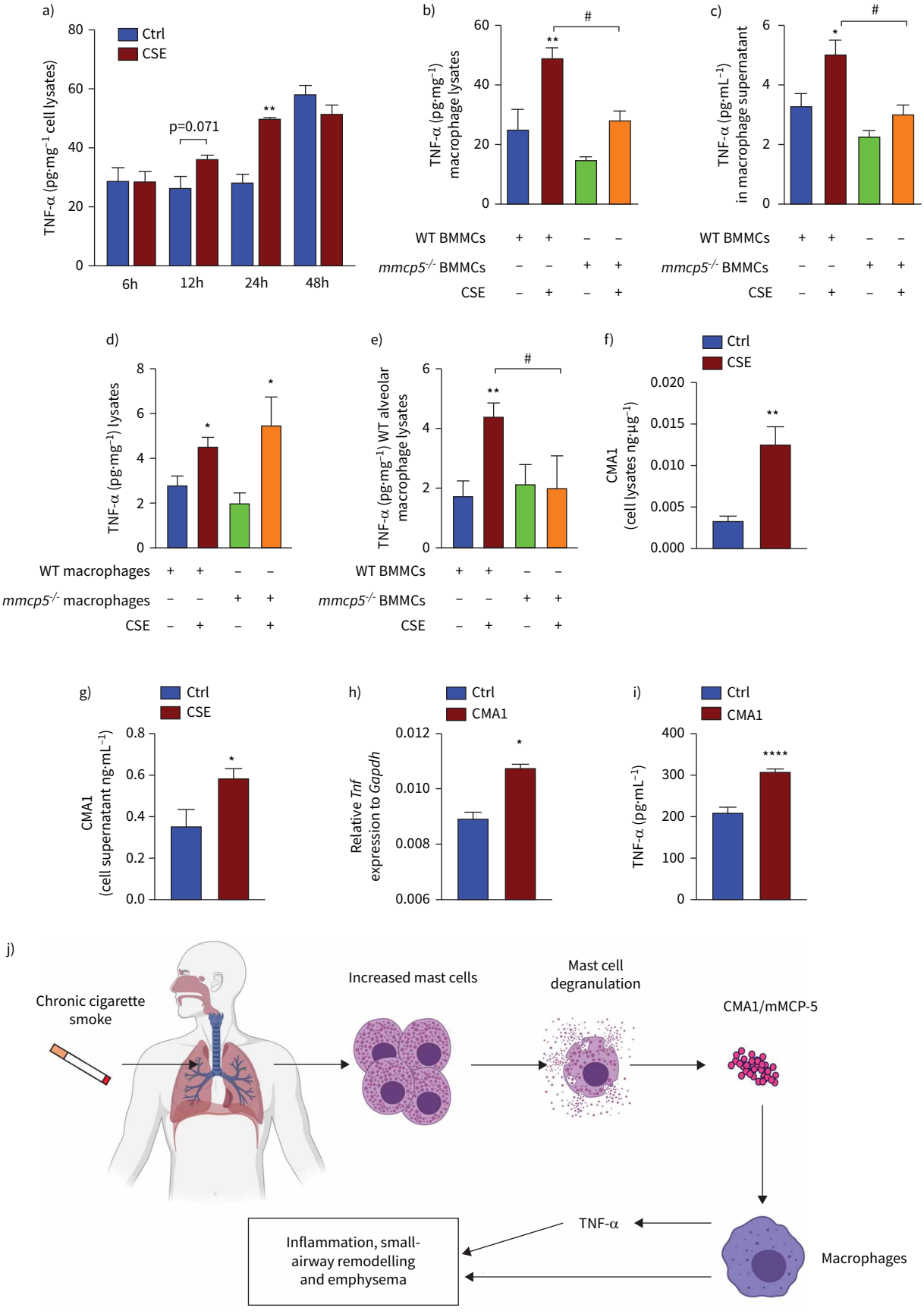
a)
Ctrl
CSE
TNF-α (pg·mg−1 cell lysates)
p=0.071
6h
12h
24h
48h
b)
TNF-α (pg·mg−1) macrophage lysates
WT BMMCs
mmcp5−/− BMMCs
CSE
c)
TNF-α (pg·mL−1) in macrophage supernatant
WT BMMCs
mmcp5−/− BMMCs
CSE
d)
TNF-α (pg·mg−1) lysates
WT macrophages
mmcp5−/− macrophages
CSE
e)
TNF-α (pg·mg−1) WT alveolar macrophage lysates
WT BMMCs
mmcp5−/− BMMCs
CSE
f)
Ctrl
CSE
CMA1 (cell lysates ng·µg−1)
g)
Ctrl
CSE
CMA1 (cell supernatant ng·mL−1)
h)
Ctrl
CMA1
Relative Tnf expression to Gapdh
i)
Ctrl
CMA1
TNF-α (pg·mL−1)
j)
Chronic cigarette smoke
Increased mast cells
Mast cell degranulation
CMA1/mMCP-5
TNF-α
Macrophages
Inflammation, small-airway remodelling and emphysema

FIGURE 7 Cigarette smoke induces CMA1 release from mast cells (MCs) which induces macrophage secretion of tumour necrosis factor (TNF)-α. a) Mouse bone marrow-derived mast cells (mBMMCs) from wild-type (WT) mice were co-cultured with mouse macrophages (RAW264.7) and exposed to 5% cigarette smoke extract (CSE) for 6, 12, 24 or 48 h. TNF-α protein levels were measured in cell lysates. mBMMCs from WT and mouse mast cell protease (*mmcp5*)$^{-/-}$ mice were co-cultured with mouse macrophages and exposed to 5% CSE for 24 h. TNF-α protein levels were measured in b) cell lysates and c) supernatants. n=3–6. d) Alveolar macrophages were isolated from WT and *mmcp5*$^{-/-}$ mice with or without 5% CSE stimulation and TNF-α protein levels measured in cell lysates. e) Alveolar macrophages from WT mice were co-cultured with mBMMCs from WT and *mmcp5*$^{-/-}$ mice with or without 24 h 5% CSE stimulation and TNF-α protein levels were measured in cell lysates. Human MCs were challenged with 5% CSE or media for 24 h and CMA1 protein was measured in f) cell lysates and g) supernatants by ELISA, n=5–6. Human macrophages (THP-1 differentiated macrophage cell line) were challenged with recombinant human (h)CMA1 protein for 24 h. h) TNF gene expression in cells by quantitative PCR. i) TNF protein levels in supernatant by ELISA. j) Pathway of MC CMA1/mMCP5 contribution to COPD. CS exposure increases MC numbers and degranulation to release CMA1/mMCP5 in the lungs. mMCP5 induces macrophage to release TNF-α that leads to lung inflammation, small-airway remodelling and empyema in COPD. Data are presented as mean±SEM. Statistical differences were determined using one-way ANOVA with Bonferroni post-test. *: p<0.05, **: p<0.01, ****: p<0.001 compared to non-CSE exposed control WT cells. #: p<0.05 compared to CSE-exposed mBMMCs from WT mice.

completely inhibited with CMA1 inhibitor treatment (figure 8a). We then treated mice with a CMA1 inhibitor for 6–8 weeks of CS exposure to test the therapeutic potential. The CMA1 inhibitor had potent effects and suppressed all of the hallmark features of experimental COPD. Treatment suppressed chronic airway inflammation and reduced total leukocytes, predominantly macrophages, neutrophils and lymphocytes in BALF after 8 weeks CS exposure (figure 8b–e). Treatment also almost completely suppressed airway fibrosis and collagen deposition around the small airways (figure 8f and g) and emphysema-like alveolar enlargement (figure 8h and i) back to baseline in air-exposed controls in both cases. Treatment also prevented decreases in lung function in terms of lung volume, dynamic compliance and static lung compliance (figure 8j–l) again back to baseline levels in air-exposed controls.

Discussion

We show for the first time that mast cell-derived CMA1/mMCP5 contributes to COPD pathogenesis. *hCMA1* mRNA is expressed at higher levels and CMA1^{+} mast cells are increased in the lungs of COPD patients. Lung mCMA1/mMCP5 protein, mast cells and mMCP5^{+} mast cells are increased in experimental COPD. We developed *mmcp5*$^{-/-}$ mice and showed that mMCP5 has a prominent deleterious role in experimental COPD. *mmcp5* deficiency protects against pulmonary inflammation, airway remodelling, emphysema and impaired lung function in experimental COPD. Notably, treatment with a CMA1 inhibitor potently suppressed these hallmark features of experimental COPD. Finally, we define the mechanism whereby CS induces CMA1 release that in turn induces TNF-α secretion from macrophages.

COPD is a progressive disease, and CS-induced inflammation is a primary driver of pathogenesis. Mast cells have potent effects on immunity through degranulation and secretion of potent mediators: chymases, tryptases and others. They have important roles in lung disorders, particularly asthma, and, as we now show, in COPD. We are the first to show increased *hCMA1* mRNA expression in lung biopsies from severe COPD patients, indicating that it is associated with increased disease severity. Previous studies showed that hCMA1^{+} mast cells are increased in COPD lungs compared to healthy donors [17, 31]. Some reported that they are resident around blood vessels [17], whereas others showed that they were mainly located around airway smooth muscle in COPD lungs [31].

We found that degranulated mast cells were also increased in the lungs of wild-type mice with CS-induced experimental COPD, confirming that pulmonary mast cell are activated. We also found increased mMCP5 protein levels in experimental COPD lungs, in line with increased *hCMA1* mRNA levels and CMA1^{+} mast cells in patient lungs. We also found that CMA1^{+} mast cells were in the parenchyma in controls, but around blood vessels and airways in experimental COPD.

Using *mmcp5*$^{-/-}$ C57BL/6 mice, we demonstrate critical roles for mMCP5 in experimental COPD through driving pulmonary macrophage and TNF-α responses. We previously showed that *mmcp5*$^{-/-}$ mice have reduced pathology in experimental arthritis [12], supporting our current findings that mMCP5 regulates mast cell-dependent inflammation. Mast cells express a diverse array of pro- and anti-inflammatory responses. Our previous studies revealed that mast cells have potent pro-inflammatory activity in response to particulate insults. Mice deficient in other mast cell proteases (*e.g.* mMCP6 homologue of human tryptase-β, and Prss31 homologue of human tryptase-γ) were partially protected from inflammation and small airway remodelling in experimental CS-induced COPD [9]. However, other studies show that mast cells can suppress inflammation in other contexts [36]. Mast cells protect mice against bacterial and viral

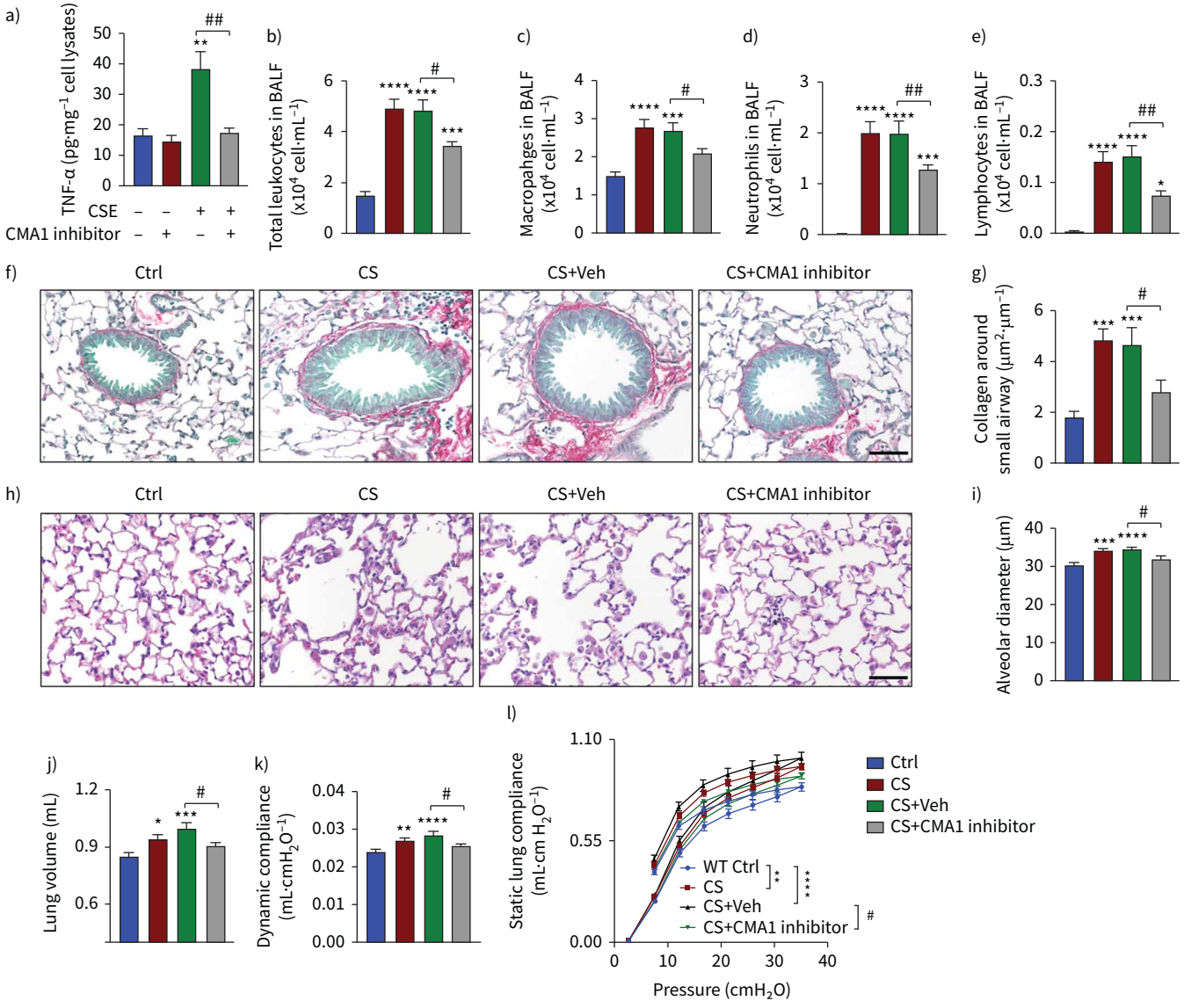

FIGURE 8 Chymase (CMA)1 inhibitor suppresses the hallmark features of experimental COPD. a) Bone marrow derived mast cells were challenged with cigarette smoke extract (CSE) or media and treated with or without CMA1 inhibitor, tumour necrosis factor (TNF) levels were assessed in cell lysates. WT mice were exposed to cigarette smoke (CS) for 8 weeks, controls (Ctrl) were exposed to normal air. Some mice were treated with CMA1 inhibitor intranasally from week 6 to week 8 of CS exposure and vehicle (Veh)-treated controls received an equal volume of PBS. Total b) leukocytes, c) macrophages, d) neutrophils and e) lymphocytes in bronchoalveolar lavage fluid (BALF). f) Mouse lungs were stained with Sirius Red and Fast Green for collagen (scale bar=50 μm) and g) collagen deposition around small airways was normalised to the perimeter of basement membrane. h) Mouse lung sections were stained with haematoxylin and eosin (scale bar=50 μm) and i) alveolar diameter was determined using mean linear intercept. Mouse lung function in terms of j) lung volume, k) dynamic compliance and l) static lung compliance from pressure–volume loops. n=8. Data are presented as mean±SEM. Statistical differences were determined using one-way ANOVA with Bonferroni post-test. *: p<0.05, **: p<0.01, ***: p<0.001, ****: p<0.0001 compared to air-exposed controls. #: p<0.05, ##: p<0.01 compared to vehicle-treated CS-exposed controls.

infection and *Mycoplasma pulmonis*-induced pneumonia, and infected mast cell-deficient mice die due to a lack of protective immunity [37].

We confirmed that lung TNF-α mRNA expression and protein levels are increased in CS-induced experimental COPD and show critical roles for mMCP5 in driving these responses using *mmcp5*$^{-/-}$ mice. Previous studies show that TNF-α protein was increased in macrophages after CSE challenge [38]. In this study, TNF-α protein levels were also increased in co-cultured macrophages after CSE challenge. We also show that this TNF-α protein release from macrophages was increased after co-culture with mast cells from

wild-type but not *mmcp5*$^{-/-}$ mice when exposed to CSE. TNF-α is an important pro-inflammatory cytokine in COPD with critical roles in inflammatory cell recruitment and tissue remodelling [39]. TNF-α mRNA and protein levels are increased in COPD patients, and macrophages are the primary lung cell source [33]. Together these findings provide strong evidence that mMCP5 regulates TNF-α production from macrophages in experimental COPD. Further studies are needed to define the molecular mechanisms involved and the contributions of other myeloid cells.

The reduction in inflammatory responses in *mmcp*$^{-/-}$ mice resulted in the complete inhibition of airway fibrosis and emphysema. Further studies need to deduce how mMCP5 promotes these effects. h/mCMA1 and h/mCPA3 are stored in the secretory granules of mast cells in a 1:1 ratio. This is because pro-mCMA1/pro-mMCP5 forms a binary complex in the endoplasmic reticulum of mast cells. Thus, target disruption of the *mmcp5* gene adversely impacts the levels of mCPA3 in murine mast cells [12]. It is therefore possible that mMCP5 participates indirectly in experimental COPD by reducing mCPA3 protein levels in pulmonary mast cells.

Previous studies demonstrated that mast cells increase collagen production by inducing lung fibroblast proliferation [40] leading to small-airway remodelling in COPD [9]. We previously showed that ischaemia–reperfusion injury of skeletal muscle is reduced in *mmcp5*$^{-/-}$ compared to wild-type mice, further supporting prominent roles for CMA1/mMCP5 in connective tissue remodelling [41]. TNF-α contributes to lung remodelling and tissue repair and induces collagen synthesis [42]. The lack of TNF-α in *mmcp5*$^{-/-}$ mice prevents collagen deposition around the small airways. However, mMCP5 also regulates the expression and processing of certain MMP zymogens that control the deposition and cleavage of collagen and other remodelling proteins. mMCP5 has similar functional roles in inducing tissue damage in the skin. Tight junctions are decreased in *mmcp5*$^{-/-}$ mice in an experimental model of thermal skin injury compared to wild-type mice [43]. MMPs also contribute to tissue destruction in the lungs by cleaving structural proteins leading to emphysema [32]. We previously showed that compound 48/80-induced mast cell degranulation results in an increase of MMP-9 protein in the peritoneal cavity of wild-type mice, but this is reduced in *mmcp5*$^{-/-}$ mice [12]. In this study, we also found CS-induced increases in pro- and active MMP9 protein in wild-type mice that was prevented by the absence of mMCP5. These data suggest that mMCP5 contributes to MMP activation to induce fibrosis and emphysema and its inhibition may protect against these pathogenic features.

Lung function measurements are used to identify structural and functional changes in COPD patients. We established that increased transpulmonary resistance, lung volume and compliance occur in experimental COPD [3]. *mmcp5*$^{-/-}$ mice were protected against CS-induced transpulmonary resistance and compliance, which further confirm protection against small airway remodelling and emphysema, respectively. Increased lung volumes are associated with emphysema that result from the destruction of alveolar walls [44]. Transpulmonary resistance is a measure of airway and lung constriction. Small-airway remodelling and alveolar wall thickening increase transpulmonary resistance [45]. Dynamic compliance is a measure of airways and parenchyma elasticity and lung distention during breathing [46]. Static compliance reflects the elasticity of the parenchyma [47].

Previous studies show that the CMA1 inhibitor (RO5066852) reduced atherosclerotic plaque progression [48], but the effect of this inhibitor has not been tested in lung diseases. We are the first to show that this pharmaceutical CMA1 inhibitor potently reduces inflammation, small airway remodelling, emphysema and improved lung function in an experimental model of CS-induced COPD in mice. We also show that this CMA1 inhibitor reduces mast cells induced TNF protein after CSE challenge, indicating CMA1 is a potential therapeutic target and that inhibitors could be a potential treatment for COPD.

Tryptases are serine proteinases. Tetramer-forming hTryptase-β and membrane hTryptase-γ are the most abundant in human mast cells [49]. We previously showed that TNF-α protein levels were increased in lysates of bone marrow-derived macrophages exposed to recombinant hTryptase-β [8]. We also showed that *mmcp6*$^{-/-}$ mice had reduced airway inflammation and lung *Tnfa* mRNA levels compared to wild-type mice in CS-induced experimental COPD [8]. Furthermore, *Prss31*$^{-/-}$ mice had significantly reduced CS-induced airway inflammation and remodelling [9].

Collectively, this and previous studies show that several mast cell granule proteases have potent adverse effects in driving disease. It is important to define which are more significant in a particular disease and develop specific inhibitors against them as therapies. It may be necessary to suppress multiple proteases, which could be achieved with either combination therapies, inhibitors of mast cell degranulation or modifying the serglycin proteoglycans needed to maintain mast cell proteases in active conformations in

order to function. These issues should be elucidated in future studies. Nevertheless, we show potent effects of specifically inhibiting mCMA1/mMCP5 in the suppression of the hallmark features of experimental COPD. We show that CS increases mast cell numbers and degranulation to release mMCP5. mMCP5 then induces macrophages to release TNF-α in the lung, leading to inflammation, airway remodelling, emphysema and impaired lung function in COPD (figure 7j). Inhibiting mMCP5 levels and activity reduces lung inflammation, airway remodelling, emphysema and impaired lung function. Inhibiting hCMA1 may be a new therapeutic option for COPD.

Acknowledgements: We thank Duc Nguyen, Nisha Panth and Christina Nalkurthi (Center for Inflammation, Centenary Institute and University of Technology Sydney, Australia) for technical assistance. We thank Roche for permission to use and provision of RO5066852-000-006.

Author contributions: G. Liu performed most of the *in vitro* and *in vivo* experiments. K.R. Paudel, A.M. Philp, A.G. Jarnicki, M. Fricker and K. Dua performed *in vivo* experiments. W. Lu, M.S. Eapen and S.S. Sohal performed human immunohistochemistry. R. Wadhwa and V. Malyla assisted *in vitro* experiments. H. Van Eeckhoutte and K. Bracke performed qPCR in human samples. J.E. Marshall assisted immunoblot. A. Katsifis assisted qPCR in mice. N.Z. Kermani and I.M. Adcock performed sc-RNA-seq analysis. K.F. Chung, G. Caramori, A. Tiotiu and I.M. Adcock assisted in dataset analysis. G. Liu and P.M. Hansbro designed the experiments. P.M. Hansbro, P.A. Wark and B.G. Oliver revised the manuscript. P.M. Hansbro funded the experiments. All authors read and approved the manuscript.

Conflict of interest: M. Fricker reports grants from GlaxoSmithKline, outside the submitted work. P.M. Hansbro reports grants from National Health and Medical Research Council, grants from Australian Research Council, during the conduct of the study. The remaining authors disclose no potential conflicts of interest.

Support statement: P.M. Hansbro is supported by a fellowship and grants from the National Health and Medical Research Council of Australia (NHMRC #1079187, #1175134), Australian Research Council (#150102153), and the University of Technology Sydney. G. Liu is supported by CREATE Hope Scientific Fellowship and grants from Lung Foundation Australia. S.S. Sohal is supported by grants from Clifford Craig Foundation Launceston General Hospital.

References

1 GBD Chronic Respiratory Disease Collaborators. Prevalence and attributable health burden of chronic respiratory diseases, 1990–2017: a systematic analysis for the Global Burden of Disease Study 2017. *Lancet Respir Med* 2020; 8: 585-596.
2 Budden KF, Gellatly SL, Wood DL, *et al.* Emerging pathogenic links between microbiota and the gut-lung axis. *Nat Rev Microbiol* 2017; 15: 55–63.
3 Liu G, Cooley MA, Jarnicki AG, *et al.* Fibulin-1 regulates the pathogenesis of tissue remodeling in respiratory diseases. *JCI Insight* 2016; 1: e86380.
4 Budden KF, Shukla SD, Rehman SF, *et al.* Functional effects of the microbiota in chronic respiratory disease. *Lancet Respir Med* 2019; 7: 907–920.
5 Krystel-Whittemore M, Dileepan KN, Wood JG. Mast cell: a multi-functional master cell. *Front Immunol* 2015; 6: 620.
6 Wang Y, Xu J, Meng Y, *et al.* Role of inflammatory cells in airway remodeling in COPD. *Int J Chron Obstruct Pulmon Dis* 2018; 13: 3341–3348.
7 Hamilton MJ, Frei SM, Stevens RL. The multifaceted mast cell in inflammatory bowel disease. *Inflamm Bowel Dis* 2014; 20: 2364–2378.
8 Beckett EL, Stevens RL, Jarnicki AG, *et al.* A new short-term mouse model of chronic obstructive pulmonary disease identifies a role for mast cell tryptase in pathogenesis. *J Allergy Clin Immunol* 2013; 131: 752–762.
9 Hansbro PM, Hamilton MJ, Fricker M, *et al.* Importance of mast cell Prss31/transmembrane tryptase/tryptase-γ in lung function and experimental chronic obstructive pulmonary disease and colitis. *J Biol Chem* 2014; 289: 18214–18227.
10 Lu Z, Van Eekhoutte HP, Liu G, *et al.* Necroptosis signalling promotes inflammation, airway remodelling and emphysema in COPD. *Am J Respir Crit Care Med* 2021; 204: 667–681.
11 Starkey MR, Plank MW, Casolari P, *et al.* IL-22 and its receptors are increased in human and experimental COPD and contribute to pathogenesis. *Eur Respir J* 2019; 54: 1800174.
12 Stevens RL, McNeil HP, Wensing LA, *et al.* Experimental arthritis is dependent on mouse mast cell protease-5. *J Biol Chem* 2017; 292: 5392–5404.
13 Pejler G, Rönnberg E, Waern I, *et al.* Mast cell proteases: multifaceted regulators of inflammatory disease. *Blood* 2010; 115: 4981–4990.

14 Beghdadi W, Madjene LC, Claver J, *et al.* Mast cell chymase protects against renal fibrosis in murine unilateral ureteral obstruction. *Kidney Int* 2013; 84: 317–326.
15 Ahmad S, Wei CC, Tallaj J, *et al.* Chymase mediates angiotensin-(1-12) metabolism in normal human hearts. *J Am Soc Hypertens* 2013; 7: 128–136.
16 Grashoff WF, Sont JK, Sterk PJ, *et al.* Chronic obstructive pulmonary disease: role of bronchiolar mast cells and macrophages. *Am J Pathol* 1997; 151: 1785–1790.
17 Kosanovic D, Dahal BK, Peters DM, *et al.* Histological characterization of mast cell chymase in patients with pulmonary hypertension and chronic obstructive pulmonary disease. *Pulm Circ* 2014; 4: 128–136.
18 Kosanovic D, Luitel H, Dahal BK, *et al.* Chymase: a multifunctional player in pulmonary hypertension associated with lung fibrosis. *Eur Respir J* 2015; 46: 1084–1094.
19 Xu J, Xu X, Jiang L, *et al.* SARS-CoV-2 induces transcriptional signatures in human lung epithelial cells that promote lung fibrosis. *Respir Res* 2020; 21: 182.
20 Hsu AC, Starkey MR, Hanish I, *et al.* Targeting PI3K-p110α suppresses influenza virus infection in chronic obstructive pulmonary disease. *Am J Respir Crit Care Med* 2015; 191: 1012–1023.
21 Fricker M, Goggins BJ, Mateer S, *et al.* Chronic cigarette smoke exposure induces systemic hypoxia that drives intestinal dysfunction. *JCI Insight* 2018; 3: e94040.
22 Kim RY, Sunkara KP, Bracke KR, *et al.* A microRNA-21-mediated SATB1/S100A9/NF-κB axis promotes chronic obstructive pulmonary disease pathogenesis. *Sci Transl Med* 2021; 13: eaav7223.
23 Schanin J, Gebremeskel S, Korver W, *et al.* A monoclonal antibody to Siglec-8 suppresses non-allergic airway inflammation and inhibits IgE-independent mast cell activation. *Mucosal Immunol* 2021; 14: 366–376.
24 Liu G, Cooley MA, Nair PM, *et al.* Airway remodelling and inflammation in asthma are dependent on the extracellular matrix protein fibulin-1c. *J Pathol* 2017; 243: 510–523.
25 Skerrett-Byrne DA, Bromfield EG, Murray HC, *et al.* Time-resolved proteomic profiling of cigarette smoke-induced experimental chronic obstructive pulmonary disease. *Respirology* 2021; 26: 960–973.
26 Pauwels RA, Buist AS, Calverley PM, *et al.* Global strategy for the diagnosis, management, and prevention of chronic obstructive pulmonary disease. NHLBI/WHO Global Initiative for Chronic Obstructive Lung Disease (GOLD) Workshop summary. *Am J Respir Crit Care Med* 2001; 163: 1256–1276.
27 Tilley AE, Harvey BG, Heguy A, *et al.* Down-regulation of the notch pathway in human airway epithelium in association with smoking and chronic obstructive pulmonary disease. *Am J Respir Crit Care Med* 2009; 179: 457–466.
28 Steiling K, van den Berge M, Hijazi K, *et al.* A dynamic bronchial airway gene expression signature of chronic obstructive pulmonary disease and lung function impairment. *Am J Respir Crit Care Med* 2013; 187: 933–942.
29 Jiang J, Faiz A, Berg M, *et al.* Gene signatures from scRNA-seq accurately quantify mast cells in biopsies in asthma. *Clin Exp Allergy* 2020; 50: 1428–1431.
30 Dwyer DF, Ordovas-Montanes J, Allon SJ, *et al.* Human airway mast cells proliferate and acquire distinct inflammation-driven phenotypes during type 2 inflammation. *Sci Immunol* 2021; 6: eabb7221.
31 Soltani A, Ewe YP, Lim ZS, *et al.* Mast cells in COPD airways: relationship to bronchodilator responsiveness and angiogenesis. *Eur Respir J* 2012; 39: 1361–1367.
32 Liu G, Philp AM, Corte T, *et al.* Therapeutic targets in lung tissue remodelling and fibrosis. *Pharmacol Ther* 2021; 225: 107839.
33 Parameswaran N, Patial S. Tumor necrosis factor-α signaling in macrophages. *Crit Rev Eukaryot Gene Expr* 2010; 20: 87–103.
34 Churg A, Wang RD, Tai H, *et al.* Tumor necrosis factor-α drives 70% of cigarette smoke-induced emphysema in the mouse. *Am J Respir Crit Care Med* 2004; 170: 492–498.
35 Minematsu N, Blumental-Perry A, Shapiro SD. Cigarette smoke inhibits engulfment of apoptotic cells by macrophages through inhibition of actin rearrangement. *Am J Respir Cell Mol Biol* 2011; 44: 474–482.
36 Caughey GH. Mast cell tryptases and chymases in inflammation and host defense. *Immunol Rev* 2007; 217: 141–154.
37 Xu X, Zhang D, Lyubynska N, *et al.* Mast cells protect mice from *Mycoplasma pneumonia. Am J Respir Crit Care Med* 2006; 173: 219–225.
38 Bozinovski S, Vlahos R, Zhang Y, *et al.* Carbonylation caused by cigarette smoke extract is associated with defective macrophage immunity. *Am J Respir Cell Mol Biol* 2011; 45: 229–236.
39 Aaron SD, Vandemheen KL, Maltais F, *et al.* TNFα antagonists for acute exacerbations of COPD: a randomised double-blind controlled trial. *Thorax* 2013; 68: 142–148.
40 Gosman MM, Postma DS, Vonk JM, *et al.* Association of mast cells with lung function in chronic obstructive pulmonary disease. *Respir Res* 2008; 9: 64.
41 Abonia JP, Friend DS, Austen WG, *et al.* Mast cell protease 5 mediates ischemia-reperfusion injury of mouse skeletal muscle. *J Immunol* 2005; 174: 7285–7291.
42 Theiss AL, Simmons JG, Jobin C, *et al.* Tumor necrosis factor (TNF) α increases collagen accumulation and proliferation in intestinal myofibroblasts *via* TNF receptor 2. *J Biol Chem* 2005; 280: 36099–36109.

43 Bankova LG, Lezcano C, Pejler G, *et al.* Mouse mast cell proteases 4 and 5 mediate epidermal injury through disruption of tight junctions. *J Immunol* 2014; 192: 2812–2820.

44 Washko GR, Hunninghake GM, Fernandez IE, *et al.* Lung volumes and emphysema in smokers with interstitial lung abnormalities. *N Engl J Med* 2011; 364: 897–906.

45 McNulty W, Usmani OS. Techniques of assessing small airways dysfunction. *Eur Clin Respir J* 2014; 1: 25898.

46 Jones B, Donovan C, Liu G, *et al.* Animal models of COPD: what do they tell us? *Respirology* 2017; 22: 21–32.

47 Suki B, Stamenović D, Hubmayr R. Lung parenchymal mechanics. *Compr Physiol* 2011; 1: 1317–1351.

48 Bot I, Bot M, van Heiningen SH, *et al.* Mast cell chymase inhibition reduces atherosclerotic plaque progression and improves plaque stability in ApoE$^{-/-}$ mice. *Cardiovasc Res* 2011; 89: 244–252.

49 Douaiher J, Succar J, Lancerotto L, *et al.* Development of mast cells and importance of their tryptase and chymase serine proteases in inflammation and wound healing. *Adv Immunol* 2014; 122: 211–252.